Supporting Information

Selective Extraction of Xylose from Acidic Hydrolysate - from Fundamentals to Process

Luca Ricciardi,[1] Willem Verboom,*[,1] Jean-Paul Lange,*[,2,3] and Jurriaan Huskens*[,1]

[1] Department of Molecules & Materials, MESA+ Institute for Nanotechnology, Faculty of Science & Technology, University of Twente, P.O. Box 217, 7500 AE, Enschede, The Netherlands

[2] Sustainable Process Technology group, Faculty of Science & Technology, University of Twente, P.O. Box 217, 7500 AE, Enschede, The Netherlands

[3] Shell Global Solutions International B.V., Grasweg 31, 1031 HW Amsterdam, The Netherlands

Corresponding Authors:

*(W.V.) Tel: +31-53-489-2977. E-mail: w.verboom@utwente.nl

*(J.-P.L.) Tel: +31-20-630-3428. E-mail: j.p.lange@utwente.nl

*(J.H.) Tel.: +31-53-489-2995. E-mail: j.huskens@utwente.nl

Number of pages : 15

Number of figures : 16

Number of tables : 0

Table of Contents

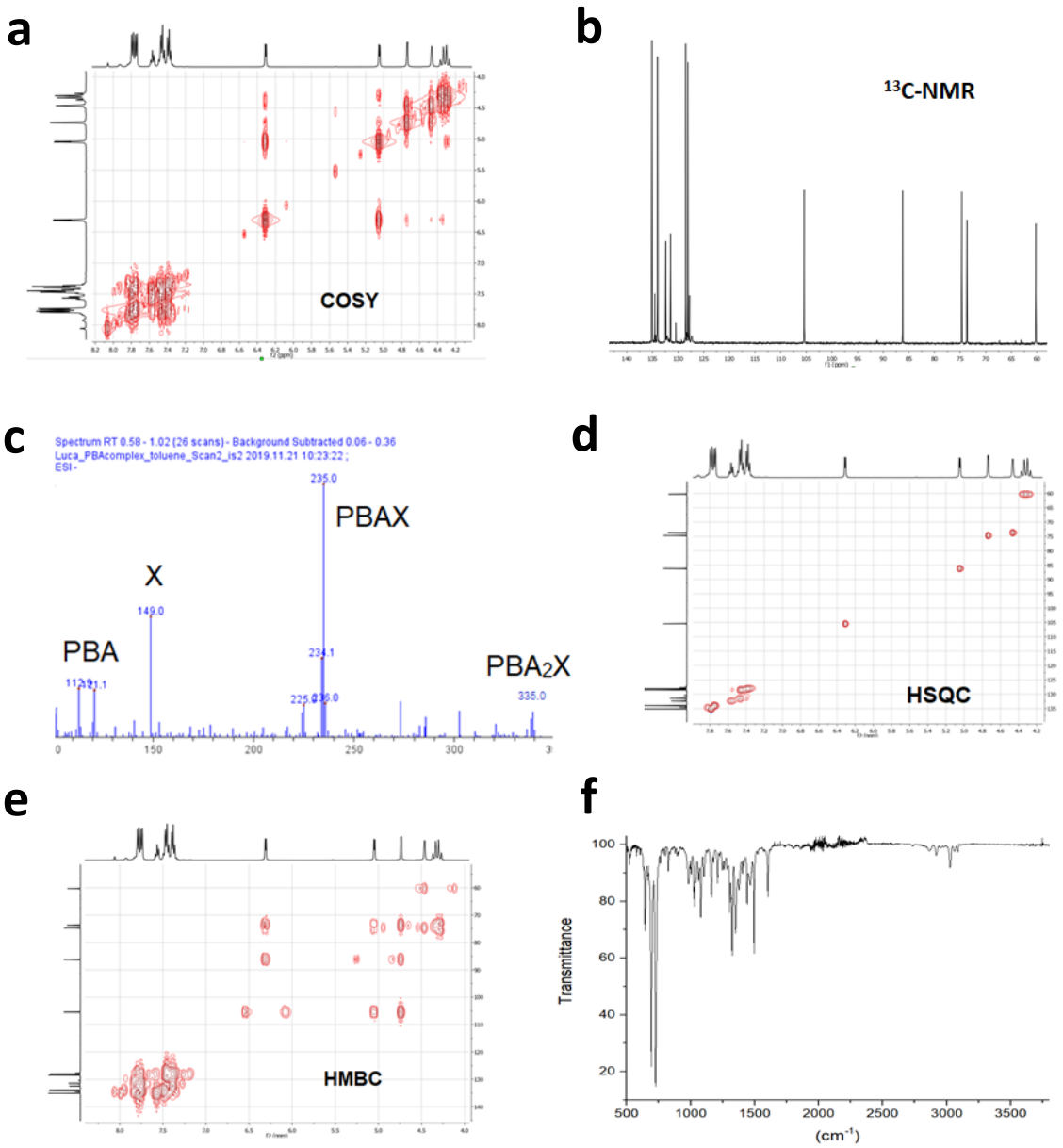

Figure S1. Characterization of PBA_2X via a) COSY homonuclear 2D NMR, b) 1D ^{13}C-NMR, c) negative ionization mode ESI mass spectrometry, d) HSQC heteronuclear 2D NMR, e) HMBC heteronuclear 2D NMR, f) FTIR spectroscopy. In particular, HSQC and HMBC show that all the protons visible in the ^{1}H-NMR spectrum can be related to a carbon, so there are no OH groups present. This can also be seen in the FTIR spectrum where no peaks at 3400 cm^{-1} are present. Mass spectrometry also shows the presence of PBA_2X and its further fragmentation to PBAX, next to free PBA and free xylose.

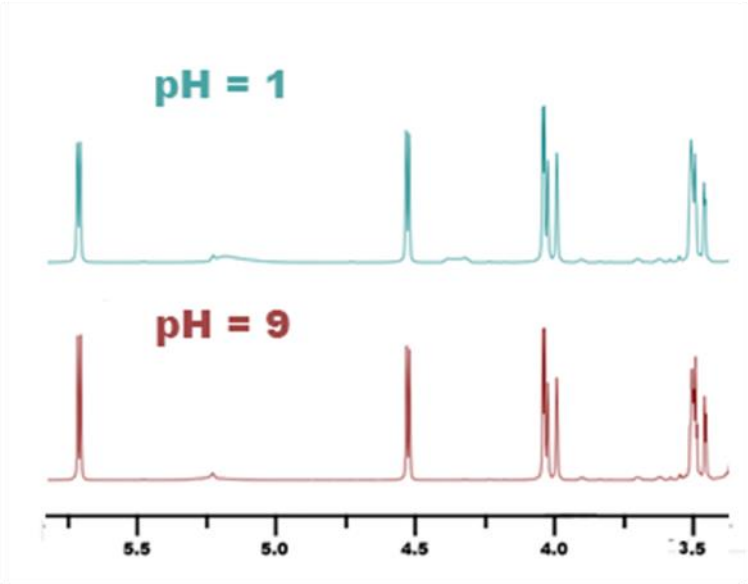

Figure S2. Comparison between the ^{1}H-NMR spectra of the toluene phases of the extraction performed at pH = 1 and pH = 9.

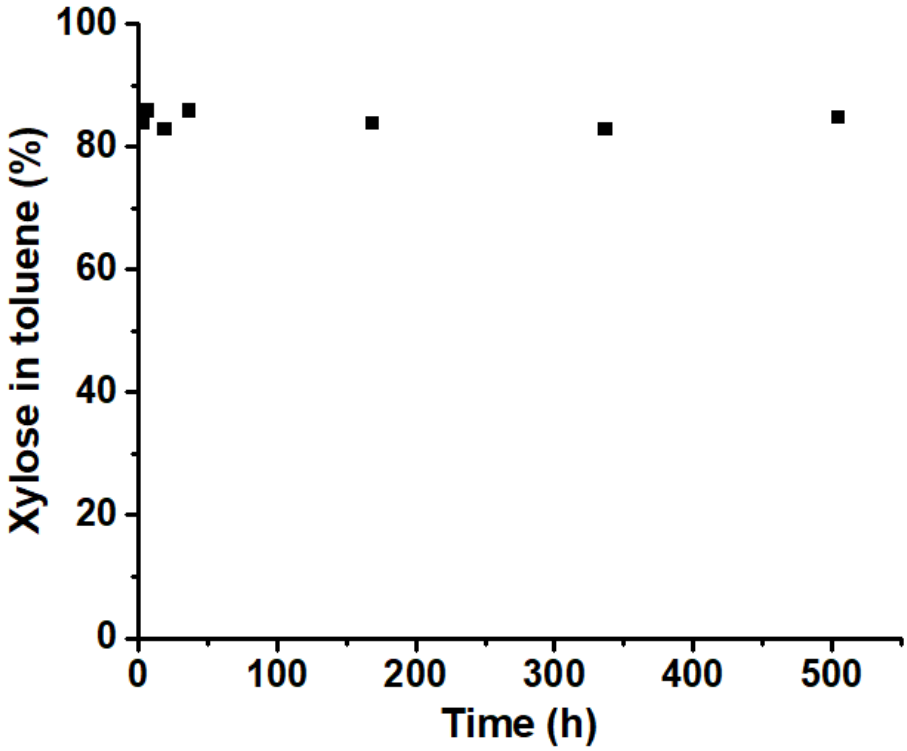

Figure S3. Stability of the partitioning of PBA_2X in a 1:1 toluene-water biphasic system over a time window of 3 weeks at room temperature.

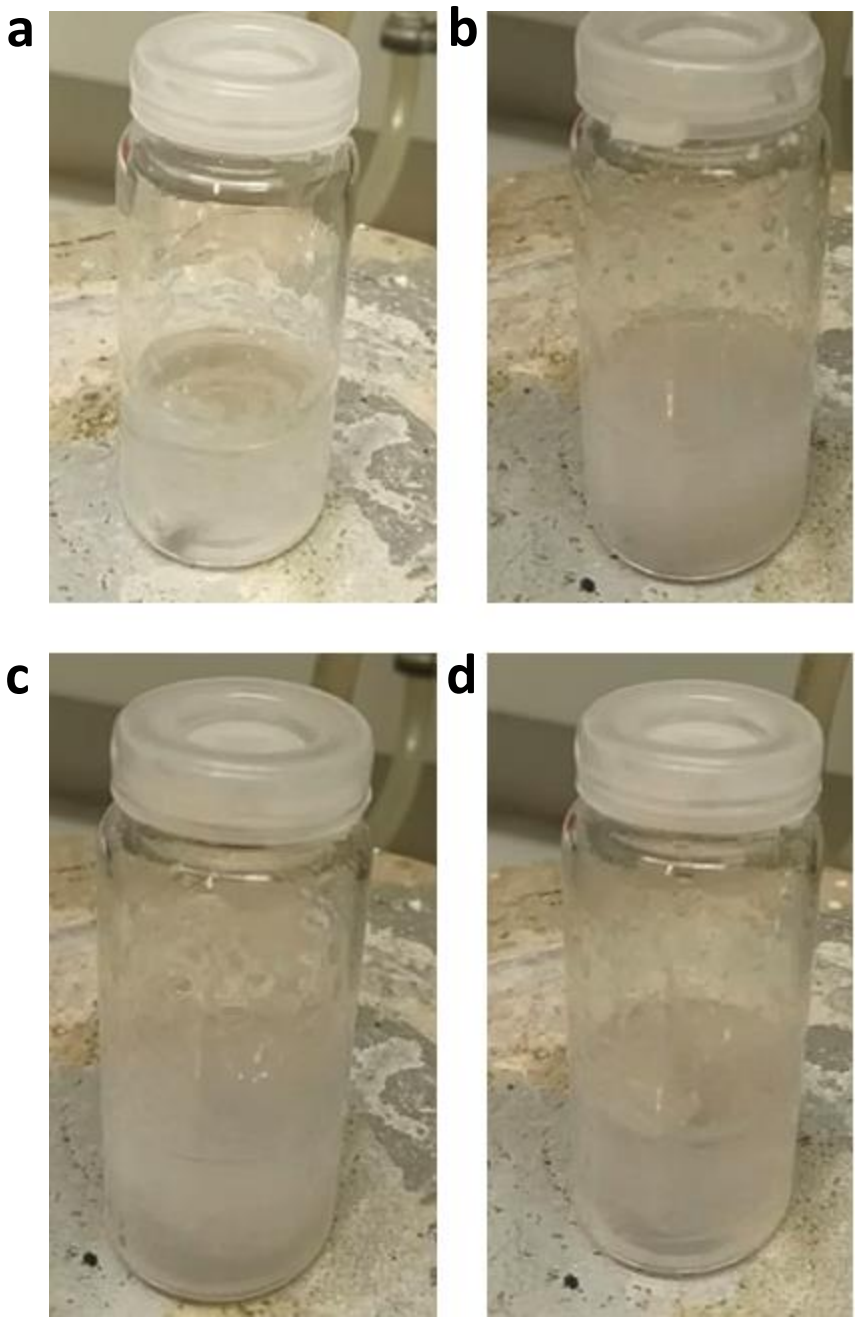

Figure S4. The extraction progresses from a) an initial phase where the two layers of the toluene-water biphasic system are clear solutions to b) a phase that starts approx. at 30 min in which turbidity starts to develop, mainly in the organic phase, c) an intermediate phase that spans approx. between 30 and 90 min where the turbidity persists, and d) a final phase that starts after approx. 90 min where the turbidity begins to disappear, resulting in a completely clear biphasic system.

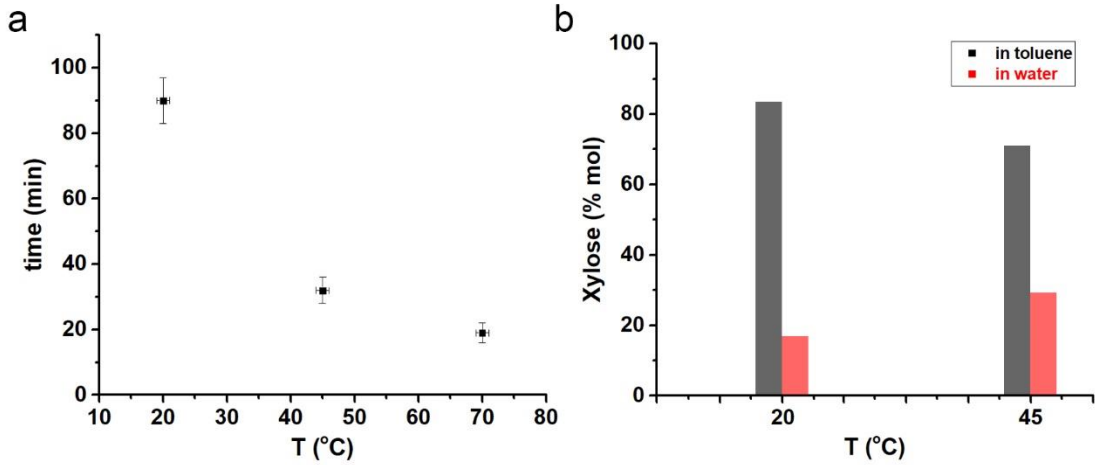

Figure S5. Xylose extraction, 1:1 toluene-water (pH = 1), starting xylose concentration 350 mM, [PBA] in toluene 700 mM, performed at temperature > 20 °C. (a) The time between the beginning of the extraction and the reaching of the equilibrium decreases when operating at higher temperatures, with the turbidity observed (Figure S4) disappearing earlier in the process. If the sampling for the analysis is done at room temperature the extraction efficiency is not influences. (b) If the sampling is performed at different temperatures the partition of the sugar in the two phases is influence, with more of the sugar residing in the aqueous phase at higher temperatures.

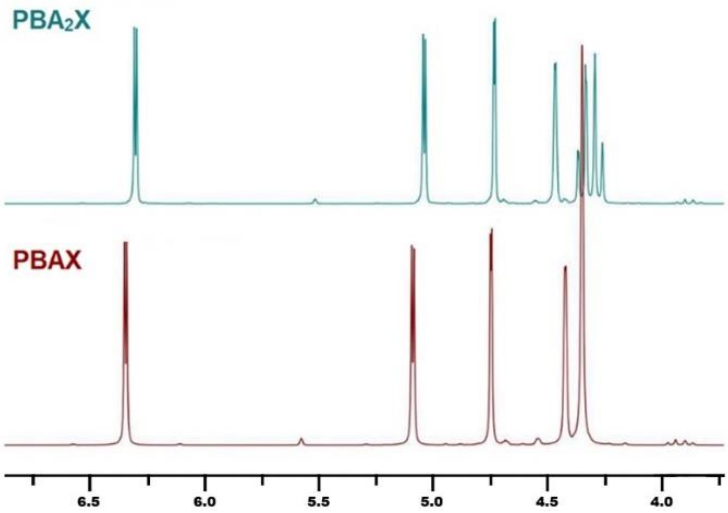

Figure S6. Comparison between the ^{1}H-NMR spectra of the PBA_2X boronate diester and the PBAX boronate monoester. Both spectra were recorded in DMSO-d_6 with the peak of DMSO (2.51 ppm) used as an internal standard.

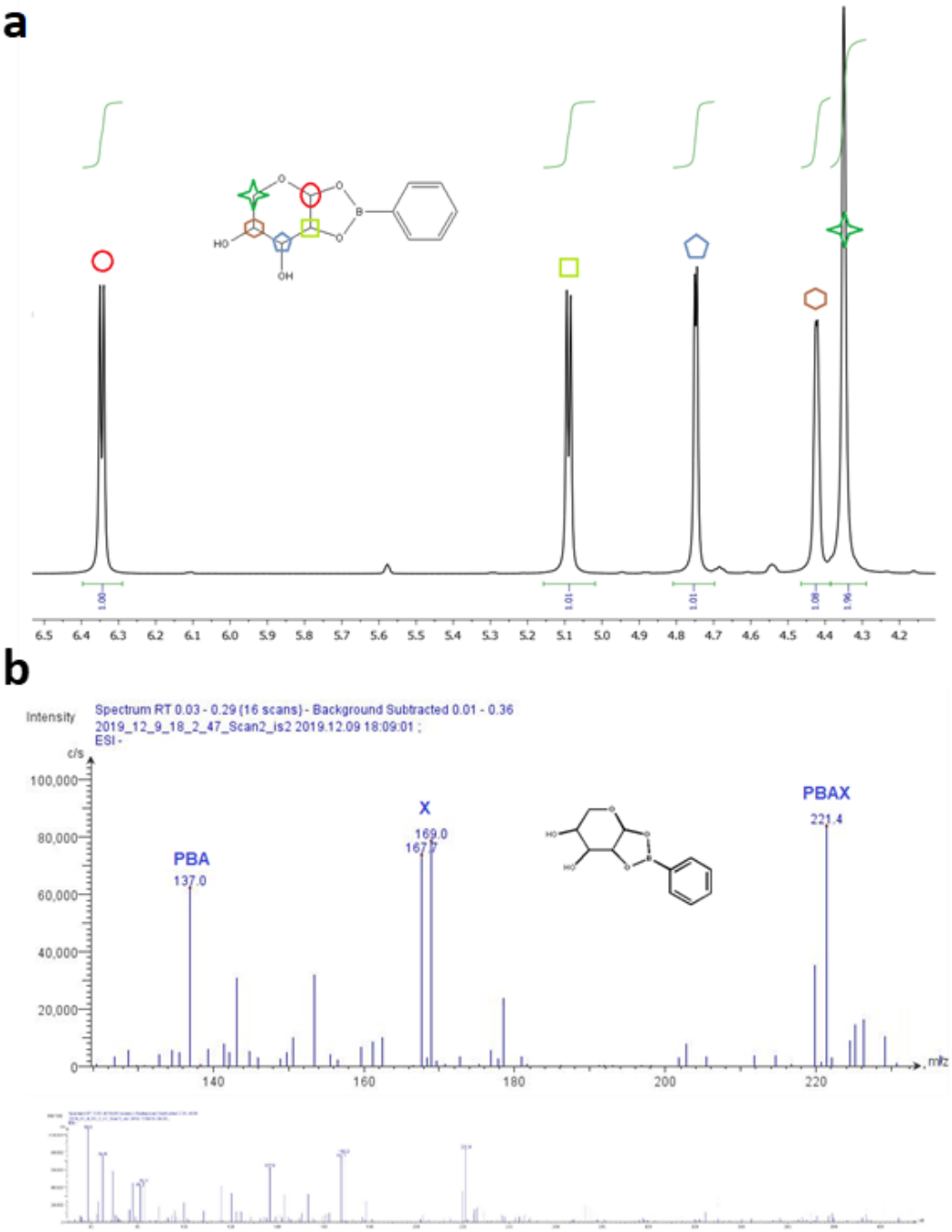

Figure S7. a) Tentative assignment of the peaks of PBAX in its ^{1}H-NMR spectrum in DMSO-d_6. The integration of the peaks observed in the region between 4 and 6.5 ppm, assuming the presence of a monoester intermediate (PBAX), shows a strong parallel with the peaks of PBA_2X. Where in the diester there is a 'quartet' for the non-anomeric protons adjacent to the oxygen atom, in the other case there is a broad singlet. This may indicate that the ring in the monoester is not as stiff as in the case of the diester, resulting in a loss in peak resolution in the spectra. The broadening and coalescence of peaks could also be an indication of ring-opening processes. In any case, all these effects are expected for the monoester and not for the diester. b) Characterization of the monoester via ESI-MS in negative mode, with the peaks of fragmentation into xylose and free PBA. A zoom out of the spectra is also provided to show no traces of the diester.

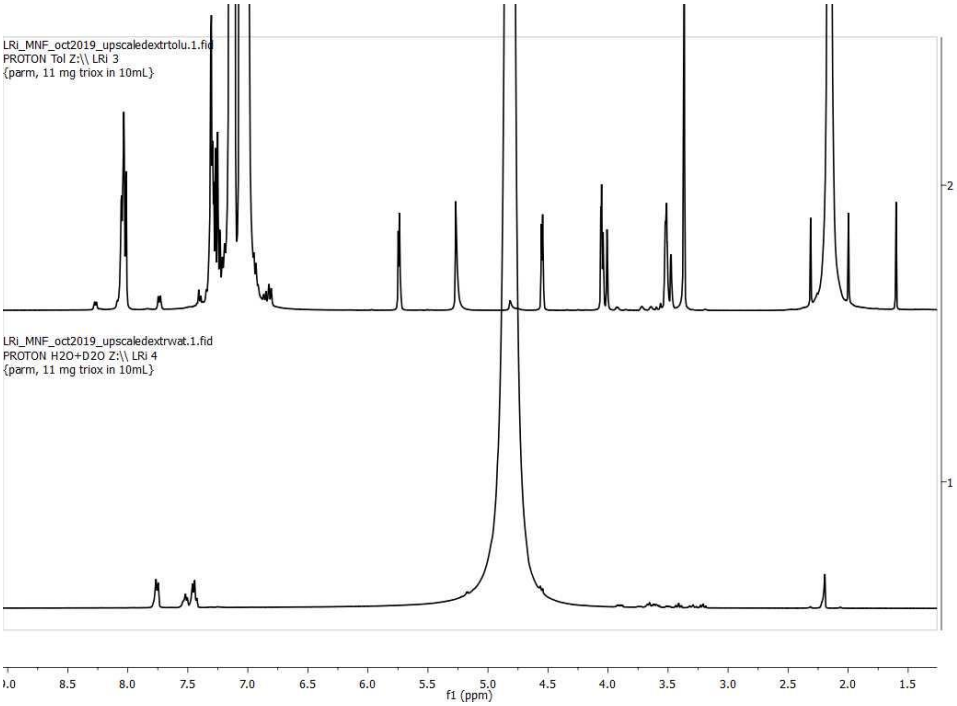

Figure S8. Partitioning of PBA in the 1:1 water-toluene system at pH = 1. Comparison between the ^{1}H-NMR of the water phase (bottom) and the toluene phase (top) after extraction.

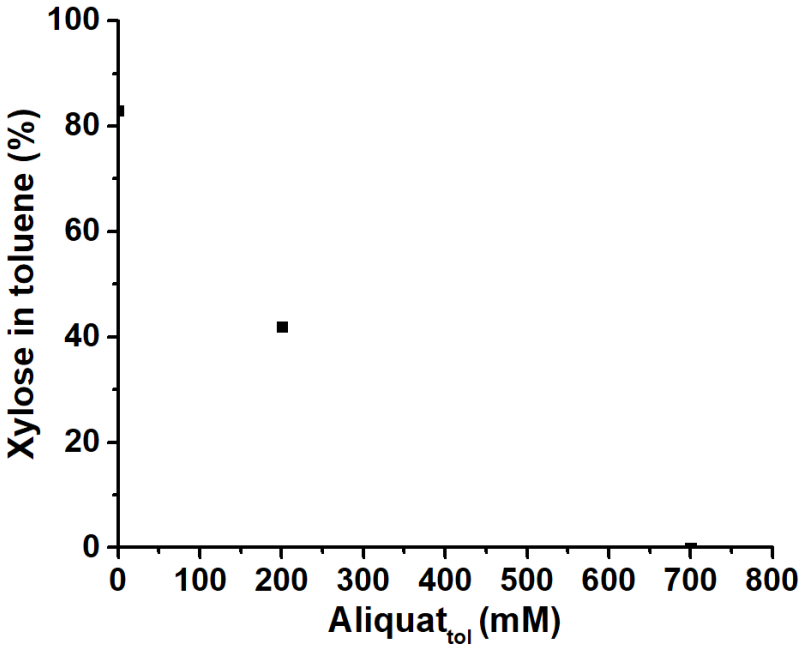

Figure S9. Xylose extraction efficiency (1:1 toluene-water, pH = 1, 350 mM xylose in water, 700 mM PBA in toluene) *vs*. Aliquat concentration in toluene.

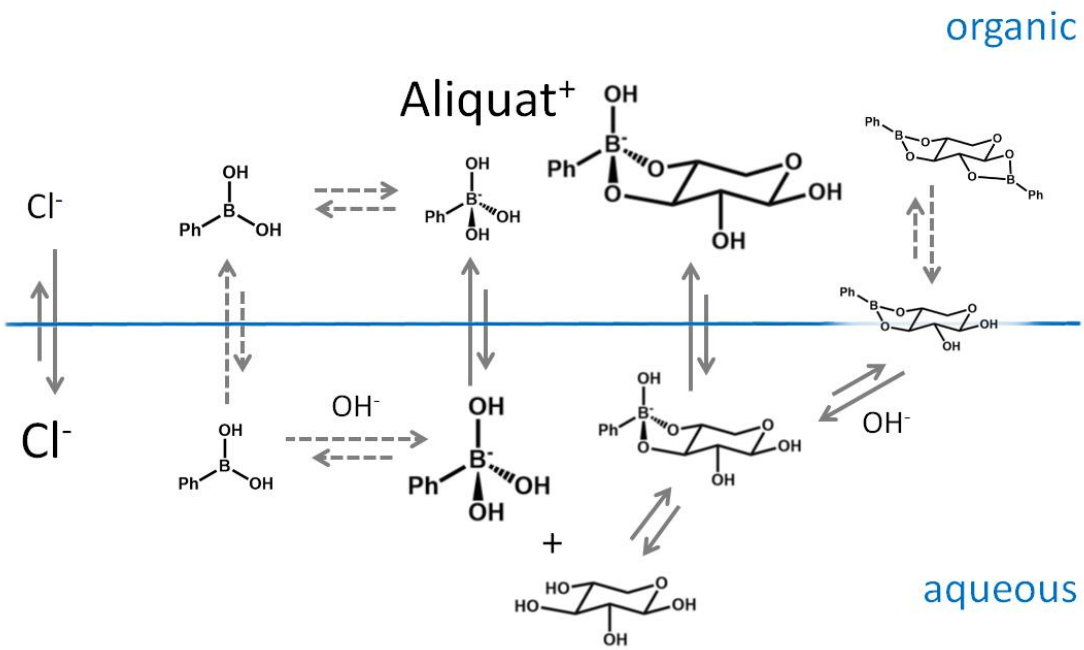

Figure S10. Common pathway of sugar extraction, where a negatively charged sugar-boronate monoester is formed in the aqueous phase and then extracted in the organic phase.

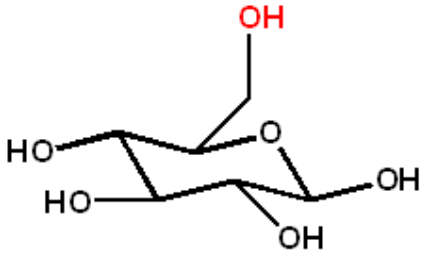

Glucose

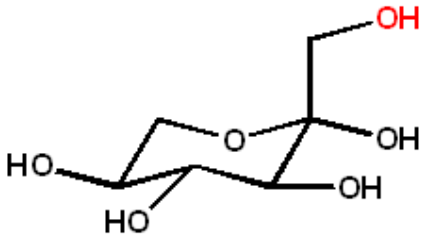

Fructose

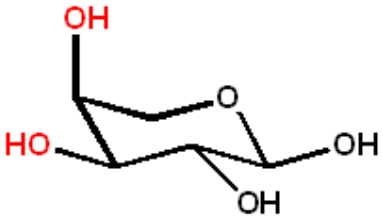

Arabinose

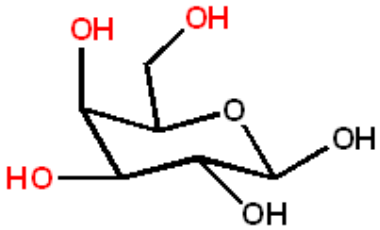

Galactose

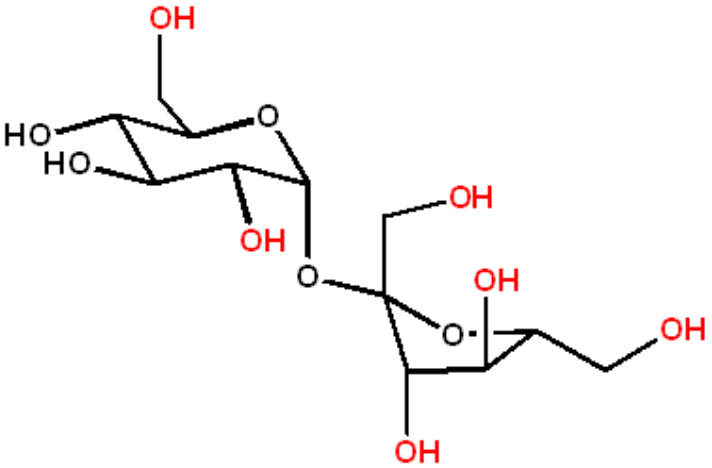

Sucrose

Figure S11. Structures of the sugars used in this study, put in the most favorable configuration for binding PBA. The OH groups that are left unbound are highlighted in red.

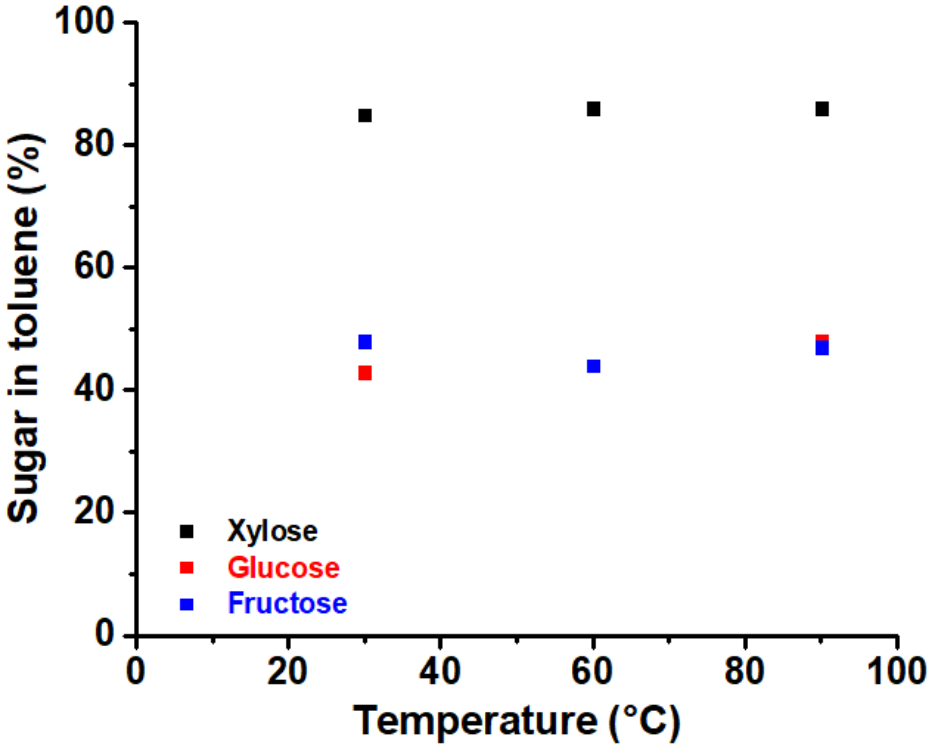

Figure S12. PBA-mediated extraction efficiency for xylose, glucose and fructose *vs.* temperature at which the extraction was performed. No effect on the final extracted sugar percentage has been observed.

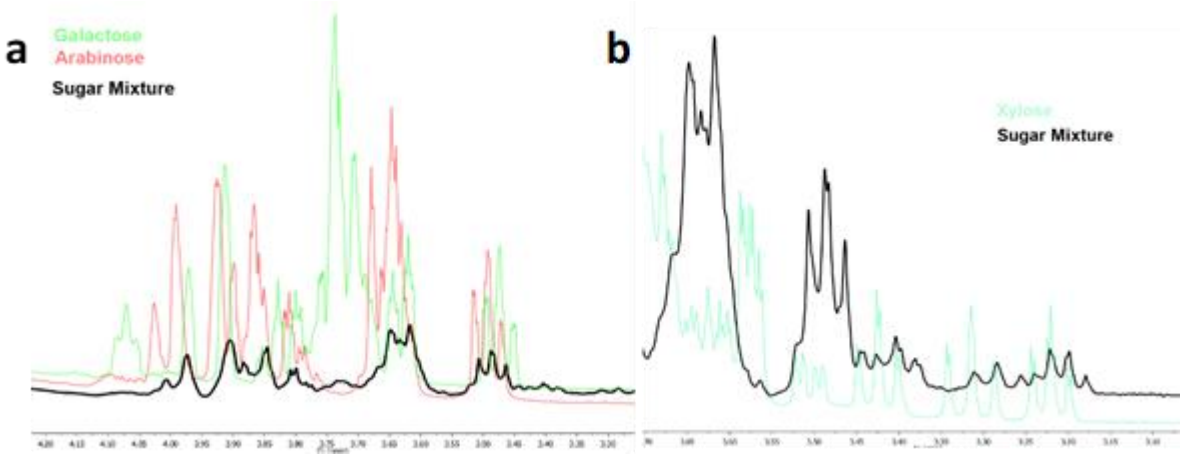

Figure S13. ^{1}H-NMR spectra of the aqueous phase (pH = 3 from acetic acid) of the sugar mixture after the extraction compared to (a) the ^{1}H-NMR spectra of arabinose and galactose and (b) the ^{1}H-NMR spectrum of xylose.

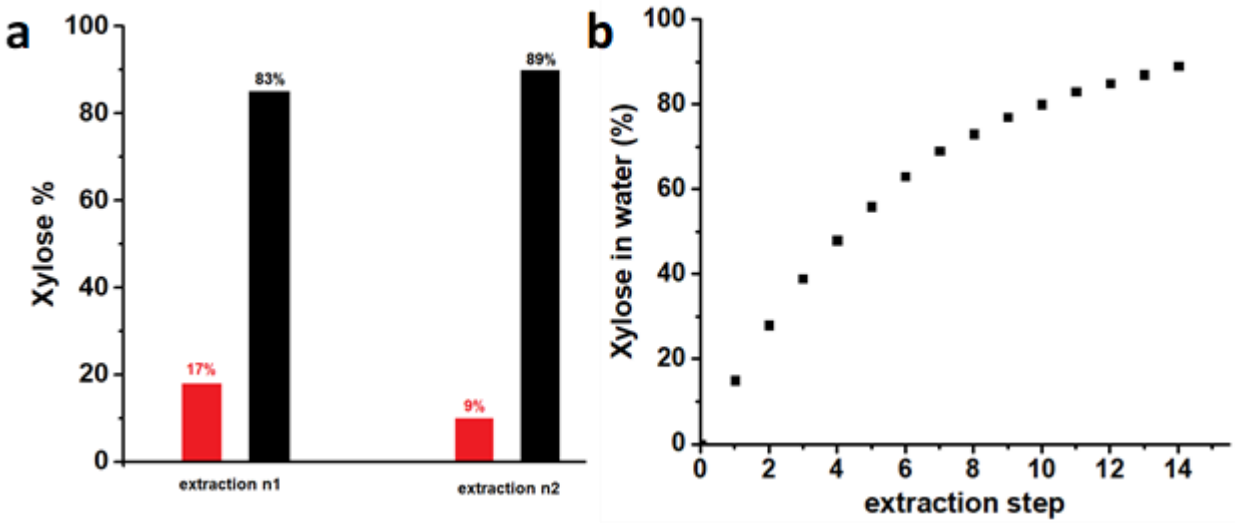

Figure S14. a) Partition of PBA_2X in a 1:1 toluene (black)-water (red) biphasic system. b) Progressive back-extraction of xylose in water in a 1:1 toluene-water biphasic system. At each step, the aqueous phase (pH = 1) is isolated and a fresh batch is re-added.

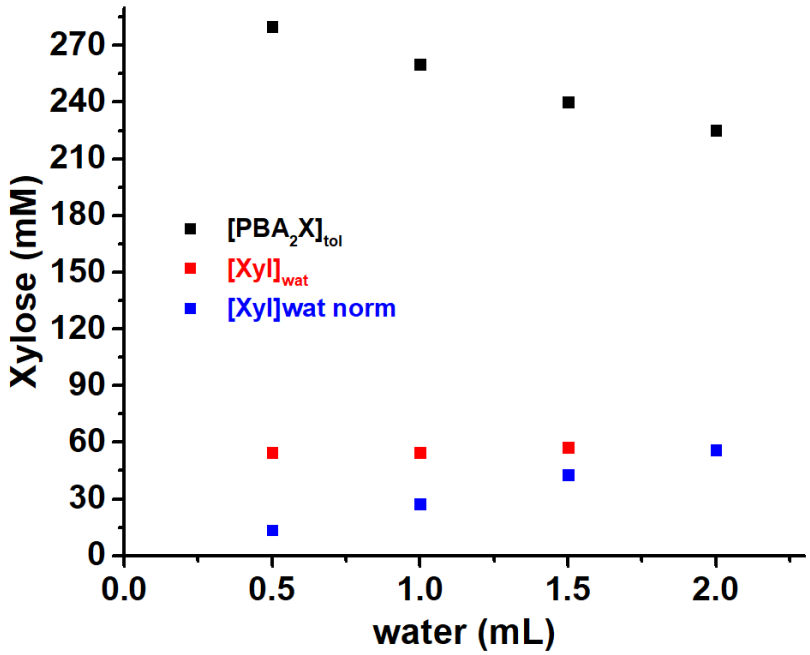

Figure S15. Xylose (in toluene and in water) mM concentrations *vs.* the amount of water used for the back-extraction of the sugar from the toluene solution of PBA_2X (2 mL). The back-extraction of xylose was performed in a biphasic system composed of a toluene solution of PBA_2X and a aqueous phase (pH = 1 from H_2SO_4). As the ratio between water and toluene is always ≤ 1, the blue dots represent the concentration 'normalized' for the volume of water used.

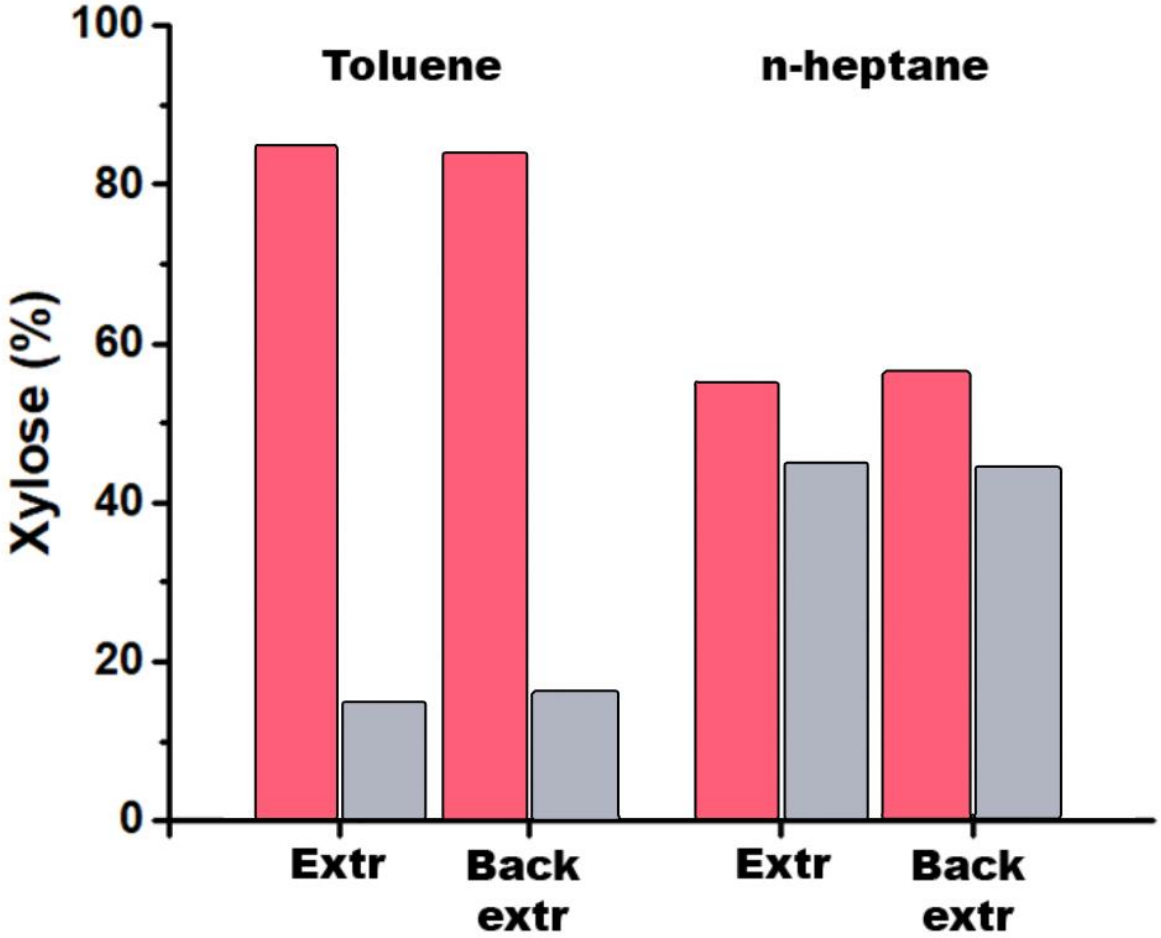

Figure S16. Comparison between the extraction and back-extraction processes performed in toluene and *n*-heptane.

Modelling Extraction and Back-Extraction

Single-stage extraction

Let's consider the extraction of a component A, from a contaminated aqueous phase to an organic one, followed by a back-extraction to a clean water phase. The thermodynamics of the extraction is characterized by the organic-water partition coefficient *K*, defined as the ratio of the concentrations of A in organic solvent, C_s, and in water, C_w (Equation S1), and the extraction efficiency *E*, which represents the ratio of the absolute amounts in both streams and is proportional to *K* and the solvent/feed ratio (Equation S2).

The extraction efficiency can then be converted into an extraction yield Y that represents the fraction of A that is extracted from the feed to the solvent stream (Equation S3). These equations are found in numerous textbooks.

$$K = \frac{Cs}{C_w}$$ Equation S1

$$E = \frac{K \cdot S}{F}$$ Equation S2

$$Y = \frac{E}{(E+1)} = \frac{KS}{KS+F}$$ Equation S3

It is less common to couple the extraction to a back-extraction to recover the solute from the solvent, particularly one that applies the same medium for back-extraction as used for the feed. But the same reasoning applies. Now, the feed of the back-extraction is the solvent, the solvent become the product stream P, and *K'* = 1/*K*.

$$E' = \frac{P}{SK}$$ Equation S4

$$Y' = \frac{E'}{(E'+1)} = \frac{P}{P+SK}$$ Equation S5

The yield after extraction and back-extraction *Y''* would then be:

$$Y'' = Y * Y' = \frac{E}{(E+1)} \cdot \frac{E'}{(E'+1)}$$ Equation S6

When P = *F*, thereby *E'* = 1/*E*, this can be simplified to:

$$Y'' = \frac{E}{(E+1)^2} = \frac{KS}{F} \frac{1}{(\frac{KS}{F}+1)^2}$$ Equation S7

Accordingly, Y'' increases with *E* = *K***S*/*F* up to a maximum of 25% for *E* = 1 and then decrease smoothly beyond *E* = 1. Higher yield can be achieved by applying multiple stages, particularly when operating them in counter-current mode.

Counter-current extraction

The overall efficiency of counter-current operation is typically expressed as the concentration ratio in solvent and feed, C_s/C_f, and related to the single-stage efficiency *E* and the number of stages n (Equation S8). This ratio can then be converted into extraction yield (Equation S9).

$$\frac{Cs}{Cf} = \frac{(E-1)}{(E^{n+1}-1)}$$ Equation S8

$$Y = 1 - \frac{Cs}{Cf} = \frac{E(E^n - 1)}{(E^{n+1} - 1)}$$ Equation S9

Applying the same reasoning to the back-extraction leads to n' stages and for the back-extraction yield to be rewritten as function of the extraction efficiency *E'*, with *E'*=1/*E* (Equation S10).

$$Y' = \frac{E'(E'^{n'} - 1)}{(E'^{n'+1} - 1)}$$ Equation S10

Consequently, the overall yield *Y''* of extraction followed by back-extraction becomes:

$$Y'' = Y \cdot Y' = \frac{(E^n - 1)}{(E^{n+1} - 1)} \frac{\left(E'^{n'} - 1\right)}{\left(E'^{n'+1} - 1\right)} = E \cdot \frac{(E^n - 1)(E^{n'} - 1)}{(E^{n+1} - 1)(E^{n'+1} - 1)}$$ Equation S11

Based on Equation S11 and its limitations (diluted feed, back-extraction in the same medium as the feed and at the same flow rate as the feed), we have calculated the overall efficiency of extraction and back-extraction in the same medium as the feed, using 20 stages to be freely distributed between extraction and back-extraction. The overall efficiency appeared to reach a maximum of 83% at single-stage *E* = *K***S*/*F* = 1 irrespective of the *K* used. The overall efficiency is also maximized by splitting the number of stages equally between extraction and back-extraction section, though the maximum efficiency is flat over a wide range of split. The efficiency further creeps to 91% for 40 stages.